

Possibility of superradiance by magnetic nanoclusters

V.I. Yukalov^{1,*} and E.P. Yukalova²

¹*Bogolubov Laboratory of Theoretical Physics,
Joint Institute for Nuclear Research, Dubna 141980, Russia*

²*Laboratory of Information Technologies,
Joint Institute for Nuclear Research, Dubna 141980, Russia*

Abstract

The possibility of realizing spin superradiance by an assembly of magnetic nanoclusters is analyzed. The known obstacles for realizing such a coherent radiation by magnetic nanoclusters are their large magnetic anisotropy, strong dephasing dipole interactions, and an essential nonuniformity of their sizes. In order to give a persuasive conclusion, a microscopic theory is developed, providing an accurate description of nanocluster spin dynamics. It is shown that, despite the obstacles, it is feasible to organize such a setup that magnetic nanoclusters would produce strong superradiant emission.

Key words: magnetic nanoclusters; coherent spin dynamics; pure spin superradiance; spin subradiance, spin induction; triggered spin superradiance

*Corresponding author e-mail: yukalov@theor.jinr.ru

1 Introduction

Coherent radiation by resonant atoms is well known and widely studied [1-5]. Different regimes of coherent optical radiation can be realized, including *superradiance* that is a self-organized coherent radiation. Quantum dots, that are called artificial atoms, can also produce superradiance [6,7], as well as several other resonant finite-level systems of different physical nature [8-12]. Spin assemblies, as such, can radiate coherently only being driven by an external magnetic field, but they cannot produce superradiance, that is a self-organized process, because of the dephasing role of their dipole spin interactions [13,14]. However, superradiance can be achieved in spin systems if they are coupled to a resonator formed by a resonant electric circuit [15]. Pure superradiance by nuclear spins was, first, observed in Dubna experiments [16-19] and later confirmed by other experimental groups [20-22]. Pulsing coherent radiation by nuclear spins, under permanent pumping, has also been observed [23-25]. The full theory of nuclear spin superradiance has been developed [26-31], being in good agreement with experiment and numerical simulations [32-34].

It is necessary to stress the principal difference between the role of particle interactions in the process of atomic and spin superradiance. Resonant atoms, by exchanging photons through the common radiation field, develop effective dipole interactions that correlate atoms, leading to the radiation coherence. So, atomic superradiance does not require the compulsory presence of a resonator. Contrary to this, dipole interactions between spins dephase spin motion, thus, resulting in their decoherence. As a result, spin superradiance cannot be realized without a resonator, whose feedback field correlates the spin motion and leads to superradiance. Additional information on atomic superradiance can be found in recent works [35-37] and the literature cited there. Superradiance by Bose-condensed atoms has also been studied [38]. The basic difference of atomic superradiance from spin superradiance is thoroughly explained in Refs. [13,14].

Nuclear spin systems are usually formed of nuclei with low spins of order $1/2$. There also exist molecular magnets, composed of identical molecules with magnetic moments of order 10 [39,40]. It has been shown theoretically [41-46] that spin superradiance can be realized by such molecular magnets.

It has also been mentioned [46] that another natural candidate for trying to realize spin superradiance would be an ensemble of magnetic nanoparticles. General properties of the latter have been reviewed in Refs. [47,48]. Magnetic particles below a critical size cannot support more than one domain and thus are described as single-domain coherent clusters. For typical material parameters, the critical diameter is between 1 – 100 nm, hence such clusters are necessarily of nanosizes. Most of the behavior of these clusters can be interpreted by treating them as objects where all magnetic moments of their internal atoms are rigidly aligned, forming a single giant spin that can reach the values as large as of order $S \sim 10^8$. If an ensemble of many such giant spins could radiate coherently, this would result in very high radiation intensity.

However, the realization of superradiance by a system of magnetic nanoparticles confronts the obstacles that seem to hinder the possibility of this realization. These obstacles are as follows. First, having large spins, these nanoparticles also have strong dipole interactions that dephase coherent spin motion. Second, magnetic nanoparticles possess rather large magnetic anisotropy, both longitudinal and transverse, which makes their effective transition frequencies time dependent, complicating by this resonance tuning [41-44]. This

is contrary to proton spins in polarized targets, having no magnetic anisotropy [49]. Third, and seemingly the most unpleasant, it is practically impossible to prepare many nanoclusters of the same size. Their sizes usually vary in a large diapason, which implies a wide spin variation. This could lead to a large nonuniform broadening suppressing coherent radiation. The broad size distribution of nanoclusters makes them principally different from magnetic molecules, all of which can be made identical to each other and forming a molecular magnet with an ideal crystalline structure.

In the present paper, the problem is studied whether it would be admissible to organize such a setup that would allow for the realization of spin superradiance by a system of magnetic nanoparticles. Since this is a rather intricate problem, the consideration, in order to be persuasive, will be based on a microscopic theory, but not on phenomenological equations.

2 Evolution of spin variables

Let us consider N nanoparticles in a sample of volume V . The microscopic spin Hamiltonian can be presented as the sum

$$\hat{H} = \sum_j \hat{H}_j + \frac{1}{2} \sum_{i \neq j} \hat{H}_{ij}, \quad (1)$$

the first term corresponding to the collection of single clusters, enumerated by the index $j = 1, 2, \dots, N$, and the second term describing their dipole interactions.

Each magnetic particle of a size below the critical one behaves as a single-domain cluster with uniform magnetization that experiences coherent rotation. Magnetic anisotropy of such a nanoparticle originates from magnetocrystalline anisotropy, from shape anisotropy that is the anisotropy of the magnetostatic energy of the sample induced by its nonspherical shape, and from surface anisotropy entering the bulk term because of the assumption of uniform magnetization. Well below the Curie temperature, the average magnetization of a cluster can be assumed to be of constant length, so that the magnetization vector rotates as a whole, which is termed the coherent rotation. These features of small single-domain particles are the basis of the Stoner-Wohlfarth model [50-52]. The quantum variant of this model can be represented by the single-cluster Hamiltonian

$$\hat{H}_j = -\mu_0 \mathbf{B} \cdot \mathbf{S}_j - D_j (S_j^z)^2 + D_{2j} (S_j^x)^2, \quad (2)$$

where $\mu_0 = -2\mu_B = -\hbar\gamma_e$, with μ_B being the Bohr magneton and γ_e , the electron gyromagnetic ratio, and where \mathbf{B} is an external magnetic field, D_j and D_{2j} are the longitudinal and transverse anisotropy parameters for a j -th cluster, and S_j^α are spin operators. Sometimes, instead of S_j^x one writes S_j^y , which is, evidently, the same.

In addition to the second-order anisotropy terms, one considers the fourth-order,

$$D_4 \left[(S_j^x)^2 (S_j^y)^2 + (S_j^y)^2 (S_j^z)^2 + (S_j^z)^2 (S_j^x)^2 \right],$$

and sixth-order,

$$D_6 (S_j^x)^2 (S_j^y)^2 (S_j^z)^2,$$

anisotropy terms. However, these terms are usually much smaller than the second-order ones and, to a good approximation, can be neglected.

The dipole interactions are described by the Hamiltonian

$$\hat{H}_{ij} = \sum_{\alpha\beta} D_{ij}^{\alpha\beta} S_i^\alpha S_j^\beta , \quad (3)$$

with the dipole tensor given by the equations

$$D_{ij}^{\alpha\beta} = \frac{\mu_0^2}{r_{ij}^3} \left(\delta_{\alpha\beta} - 3n_{ij}^\alpha n_{ij}^\beta \right) , \quad r_{ij} \equiv |\mathbf{r}_{ij}| , \quad \mathbf{n}_{ij} \equiv \frac{\mathbf{r}_{ij}}{r_{ij}} , \quad \mathbf{r}_{ij} \equiv \mathbf{r}_i - \mathbf{r}_j .$$

As has been stressed and explained in detail in Refs. [13,14,41-44], a spin system, because of the presence of dephasing dipole interactions, cannot produce superradiance without being coupled to a resonant electric circuit. It is, therefore, necessary to place the considered sample into a coil of the circuit. Then the magnetic field

$$\mathbf{B} = B_0 \mathbf{e}_z + H \mathbf{e}_x \quad (4)$$

includes, in addition to a constant external magnetic field B_0 , the feedback field H of a resonator. This feedback field is described by the Kirchhoff equation

$$\frac{dH}{dt} + 2\gamma H + \omega^2 \int_0^t H(t') dt' = -4\pi\eta \frac{dm_x}{dt} , \quad (5)$$

in which γ is the circuit damping, ω is the circuit natural frequency, $\eta = V/V_{coil}$ is a filling factor, V_{coil} is the coil volume, and

$$m_x = \frac{\mu_0}{V} \sum_j \langle S_j^x \rangle ,$$

with the angle brackets defining a statistical averaging.

For spin systems composed of proton or electron spins, it would be sufficient to tune the resonator natural frequency close to the spin Zeeman frequency

$$\omega_0 \equiv -\frac{\mu_0}{\hbar} B_0 = 2 \frac{\mu_B}{\hbar} B_0 = \gamma_e B_0 . \quad (6)$$

But for the nanoclusters, the situation is more complicated.

Deriving the evolution equations for the nanocluster spins, we will need the notation for the fluctuating spin parts

$$\begin{aligned} \xi_i^0 &\equiv \frac{1}{\hbar} \sum_{j(\neq i)} (a_{ij} S_j^z + c_{ij}^* S_j^- + c_{ij} S_j^+) , \\ \xi_i &\equiv \frac{i}{\hbar} \sum_{j(\neq i)} \left(2c_{ij} S_j^z - \frac{1}{2} a_{ij} S_j^- + 2b_{ij} S_j^+ \right) , \end{aligned} \quad (7)$$

with the relation between the spin components

$$S_j^\pm = S_j^x \pm i S_j^y , \quad S_j^x = \frac{1}{2} (S_j^+ + S_j^-) , \quad S_j^y = -\frac{i}{2} (S_j^+ - S_j^-) ,$$

and where the interaction parameters are

$$a_{ij} \equiv D_{ij}^{zz}, \quad b_{ij} \equiv \frac{1}{4} (D_{ij}^{xx} - D_{ij}^{yy} - 2iD_{ij}^{xy}), \quad c_{ij} \equiv \frac{1}{2} (D_{ij}^{xx} - iD_{ij}^{yz}).$$

Also, let us define the effective force acting on a j -th spin,

$$f_j \equiv -\frac{i}{\hbar} \mu_0 H + \xi_j. \quad (8)$$

Using the commutation relations

$$\begin{aligned} [S_i^x, S_j^y] &= i\delta_{ij} S_j^z, & [S_i^y, S_j^z] &= i\delta_{ij} S_j^x, & [S_i^z, S_j^x] &= i\delta_{ij} S_j^y, \\ [S_i^+, S_j^-] &= 2\delta_{ij} S_j^z, & [S_i^z, S_j^+] &= \delta_{ij} S_j^+, & [S_i^z, S_j^-] &= -\delta_{ij} S_j^- \end{aligned}$$

gives the following commutators involving the anisotropy terms:

$$\begin{aligned} [S_i^-, (S_j^z)^2] &= S_j^- S_j^z + S_j^z S_j^-, \\ [S_i^-, (S_j^x)^2] &= -(S_j^x S_j^z + S_j^z S_j^x), \\ [S_i^z, (S_j^x)^2] &= i(S_j^x S_j^y + S_j^y S_j^x). \end{aligned}$$

As a result, the Heisenberg equations of motion yield the equations for the spin variables, transverse,

$$\frac{dS_j^-}{dt} = -i(\omega_0 + \xi_j^0) S_j^- + f_j S_j^z + \frac{i}{\hbar} D_j (S_j^- S_j^z + S_j^z S_j^-) + \frac{i}{\hbar} D_{2j} (S_j^x S_j^z + S_j^z S_j^x), \quad (9)$$

and the longitudinal one,

$$\frac{dS_j^z}{dt} = -\frac{1}{2} (f_j^+ S_j^- + S_j^+ f_j) + \frac{1}{\hbar} D_{2j} (S_j^x S_j^y + S_j^y S_j^x). \quad (10)$$

Equation (9) shows that, if the anisotropy terms would be smaller than the term containing ω_0 , then all spins, though being different, nevertheless would rotate with the frequencies close to ω_0 . Thence the coherent spin motion could be realized.

3 Averaged equations of motion

Different nanoparticles can have different spins S_j , hence different vectors \mathbf{S}_j for which $\mathbf{S}_j^2 = S_j(S_j + 1)$. But we are interested in the coherent properties of the system, that is, in the behavior of the ensemble of nanoparticles as a whole. It is, therefore, reasonable to consider the quantities averaged over all system components. We define the average nanocluster spin

$$S \equiv \frac{1}{N} \sum_{j=1}^N S_j \quad (11)$$

and the average anisotropy constants

$$D \equiv \frac{1}{N} \sum_{j=1}^N D_j, \quad D_2 \equiv \frac{1}{N} \sum_{j=1}^N D_{2j}. \quad (12)$$

Accomplishing the statistical averaging of Eqs. (9) and (10), we keep in mind that the radiation wavelength, λ , corresponding to the Zeeman frequency ω_0 , is larger than the intercluster distance a . Under this assumption $\lambda > a$, the mean-field approximation is admissible. Thus, for spins on different sites, we set

$$\langle S_i^\alpha S_j^\beta \rangle = \langle S_i^\alpha \rangle \langle S_j^\beta \rangle \quad (i \neq j), \quad (13)$$

where α and β are arbitrary Cartesian indices. For the spins, of different components but on the same site, the correct approximation [41-44] reads as

$$\langle S_j^\alpha S_j^\beta + S_j^\beta S_j^\alpha \rangle = \left(2 - \frac{1}{S_j}\right) \langle S_j^\alpha \rangle \langle S_j^\beta \rangle \quad (\alpha \neq \beta). \quad (14)$$

This formula interpolates between the spin $S_j = 1/2$, when Eq. (14) becomes the identity $0 = 0$, since the Pauli matrices anticommute, and large spins, for which the mean-field approximation is asymptotically exact, as $S_j \rightarrow \infty$.

The averaged spin variables of interest are the *transition function*

$$u \equiv \frac{1}{SN} \sum_{j=1}^N \langle S_j^- \rangle, \quad (15)$$

the *coherence intensity*

$$w \equiv \frac{1}{S^2 N(N-1)} \sum_{i \neq j}^N \langle S_j^+ S_j^- \rangle, \quad (16)$$

and the *spin polarization*

$$s \equiv \frac{1}{SN} \sum_{j=1}^N \langle S_j^z \rangle. \quad (17)$$

To retain the attenuation effects, coming from the dipole spin interactions, one includes in the equations the dephasing rate that, taking into account saturation effects [41-44], reads as

$$\Gamma_2 = \gamma_2(1 - s^2) \quad (\gamma_2 = \rho \hbar \gamma_e^2 S), \quad (18)$$

with $\rho \equiv N/V$ being the density of nanoparticles. These nanoclusters are immersed into a matrix, whose molecules interact with spins. Thence, it is also necessary to include the related relaxation rate γ_1 . In the case of the existence of a pumping polarization mechanism, the relaxation rate is $\Gamma_1 = \gamma_1 + \gamma_1^*$, where γ_1^* is a pumping rate.

Other averaged quantities of importance are the average fluctuating fields

$$\xi_0 \equiv \frac{1}{N} \sum_{j=1}^N \langle \xi_j^0 \rangle, \quad \xi \equiv \frac{1}{N} \sum_{j=1}^N \langle \xi_j \rangle, \quad (19)$$

and the average effective force

$$f \equiv \frac{1}{N} \sum_{j=1}^N \langle f_j \rangle = -\frac{i}{\hbar} \mu_0 H + \xi. \quad (20)$$

Let us introduce the *longitudinal anisotropy frequency*

$$\omega_D \equiv (2S - 1) \frac{D}{\hbar} \quad (21)$$

and the *transverse anisotropy frequency*

$$\omega_2 \equiv (2S - 1) \frac{D_2}{\hbar} . \quad (22)$$

And let us define the *effective anisotropy frequency*

$$\omega_A \equiv \omega_D + \frac{1}{2} \omega_2 \quad (23)$$

and the *effective rotation frequency*

$$\Omega \equiv \omega_0 - \omega_{AS} . \quad (24)$$

We shall also need the notation

$$F \equiv f + \frac{i}{2} \omega_2 u^* = -\frac{i}{\hbar} \mu_0 H + \xi + \frac{i}{2} \omega_2 u^* . \quad (25)$$

Averaging Eqs. (9) and (10), we get the equations for the average variables (15) to (17):

$$\begin{aligned} \frac{du}{dt} &= -i(\Omega + \xi_0 - i\Gamma_2)u + Fs , & \frac{dw}{dt} &= -2\Gamma_2 w + (u^* F + F^* u) s , \\ \frac{ds}{dt} &= -\frac{1}{2} (u^* F + F^* u) - \Gamma_1 (s - \zeta) , \end{aligned} \quad (26)$$

where ζ is the equilibrium polarization of a single cluster.

The Kirchhoff equation (5) can be represented [26-29] as the integral *feedback equation*

$$H = -4\pi\eta \int_0^t G(t-t') \dot{m}_x(t') dt' , \quad (27)$$

with the transfer function

$$G(t) = \left[\cos(\tilde{\omega}t) - \frac{\gamma}{\tilde{\omega}} \sin(\tilde{\omega}t) \right] e^{-\gamma t} ,$$

in which $\tilde{\omega} \equiv \sqrt{\omega^2 - \gamma^2}$, and with the source term

$$\dot{m}_x \equiv \frac{1}{2} \rho \mu_0 S \frac{d}{dt} (u^* + u) .$$

As is seen from these equations, the characteristic parameter defining the strength of the feedback field is the *feedback rate*

$$\gamma_0 \equiv \frac{\pi}{\hbar} \eta \rho \mu_0^2 S . \quad (28)$$

To analyze further Eqs. (26), we employ the scale separation approach [26-30,53] that is a variant of the averaging techniques [54,55]. The fast oscillating fields (19) are treated as stochastic variables, with the stochastic averaging

$$\langle\langle \xi_0(t) \rangle\rangle = \langle\langle \xi(t) \rangle\rangle = 0 , \quad \langle\langle \xi_0(t) \xi_0(t') \rangle\rangle = 2\gamma_3 \delta(t-t') ,$$

$$\langle\langle \xi_0(t)\xi(t') \rangle\rangle = \langle\langle \xi(t)\xi(t') \rangle\rangle = 0, \quad \langle\langle \xi^*(t)\xi(t') \rangle\rangle = 2\gamma_3\delta(t-t'), \quad (29)$$

in which γ_3 is the dynamic broadening of the order of γ_2 .

Microscopic evolution equations (9) and (10), as well as the averaged equations (26), show that different spins can rotate with the approximately same frequency, close to ω_0 , only when their dipole interactions and magnetic anisotropies are sufficiently small, such that they do not disturb much the spin motion. And the feedback action of the resonator is effective, if the circuit natural frequency ω is tuned close to the Zeeman frequency ω_0 . The latter implies the resonance condition

$$\left| \frac{\Delta}{\omega} \right| \ll 1 \quad (\Delta \equiv \omega - \omega_0). \quad (30)$$

While the condition that the effective rotation frequency Ω be close to the Zeeman frequency ω_0 requires that the anisotropy be small, such that

$$\left| \frac{\omega_D}{\omega} \right| \ll 1 \quad \left| \frac{\omega_2}{\omega} \right| \ll 1. \quad (31)$$

Also, all attenuation rates are assumed to be smaller than the natural frequency ω , that is,

$$\begin{aligned} \frac{\gamma}{\omega} \ll 1, \quad \frac{\gamma_0}{\omega} \ll 1, \quad \frac{\gamma_1}{\omega} \ll 1, \\ \frac{\gamma_2}{\omega} \ll 1, \quad \frac{\gamma_3}{\omega} \ll 1. \end{aligned} \quad (32)$$

Under inequalities (32), the feedback equation (27) can be solved by iterating its right-hand side with $u(t) = u(0) \exp(-i\Omega t)$, which yields

$$\mu_0 H = i\hbar(\alpha u - \alpha^* u^*), \quad (33)$$

where the coupling function α , for a sharp resonance, such that $|\Delta/\gamma| < 1$, reads as

$$\alpha = g\gamma_2 \frac{\Omega}{\omega_0} (1 - e^{-\gamma t}), \quad (34)$$

with the dimensionless *coupling parameter*

$$g \equiv \frac{\gamma\gamma_0\omega_0}{\gamma_2(\gamma^2 + \Delta^2)}. \quad (35)$$

In what follows, we shall also need the effective coupling function

$$\tilde{\alpha} \equiv \alpha + \frac{i}{2} \omega_2. \quad (36)$$

Substituting the feedback field (33) into Eqs. (26) yields the equations

$$\frac{du}{dt} = -i(\Omega + \xi_0)u - (\Gamma_2 - \alpha s)u + \xi s - s(\tilde{\alpha}u)^*, \quad (37)$$

$$\frac{dw}{dt} = -2(\Gamma_2 - \alpha s)w + (u^*\xi + \xi^*u)s - 2s\text{Re}(\tilde{\alpha}u^2), \quad (38)$$

$$\frac{ds}{dt} = -\alpha w - \frac{1}{2}(u^* \xi + \xi^* u) - \Gamma_1(s - \zeta) + \text{Re}(\tilde{\alpha} u^2). \quad (39)$$

Complimenting these by the initial conditions $u_0 = u(0)$, $w_0 = w(0)$, $s_0 = s(0)$, without the loss of generality, one can set $u_0 = u_0^*$ to be real.

Equations (37) to (39) show that the variable u can be treated as fast, as compared to the slow variables w and s . Following the scale separation approach [26-30,53], we solve Eq. (37) for the fast variable u , keeping there the slow variables w and s as quasi-integrals of motion, which gives

$$u = u_0 \exp \left\{ -(i\Omega + \Gamma_2 - \alpha s)t - i \int_0^t \xi_0(t') dt' \right\} + s \int_0^t \xi(t') \exp \left\{ -(i\Omega + \Gamma_2 - \alpha s)(t - t') - i \int_{t'}^t \xi_0(t'') dt'' \right\} dt'.$$

Substituting this solution into Eqs. (38) and (39), we average the right-hand sides of the latter over time and over the stochastic variables (19), again keeping the slow variables fixed. In this way, we come to the equations for the guiding centers:

$$\frac{dw}{dt} = -2(\Gamma_2 - \alpha s)w + 2\gamma_3 s^2, \quad \frac{ds}{dt} = -\alpha w - \gamma_3 s - \Gamma_1(s - \zeta). \quad (40)$$

4 Coherent radiation by nanoclusters

We shall study the derived equations (40), setting there $\zeta = -1$, assuming the exact resonance, with $\Delta = 0$, and measuring time in units of $1/\gamma_2$. Then Eqs. (40) reduce to

$$\frac{dw}{dt} = -2(1 - s^2 - \alpha s)w + 2\gamma_3 s^2, \quad \frac{ds}{dt} = -\alpha w - \gamma_3 s - \gamma_1(s + 1). \quad (41)$$

The coupling function (34) can be written as

$$\alpha = g(1 - As) (1 - e^{-\gamma t}), \quad (42)$$

where the *anisotropy parameter* is

$$A \equiv \frac{\omega_A}{\omega_0}. \quad (43)$$

Solving these equations, we can calculate the radiation intensity

$$I_S(t) = \frac{2\mu_0^2}{3c^3} \left| \sum_i \langle \ddot{S}_j(t) \rangle \right|^2,$$

due to spin radiation, and the time-averaged intensity

$$\bar{I}_S(t) = \frac{2\mu_0^2}{3c^3} N^2 S^2 \Omega^4 w(t).$$

It is convenient to define the dimensionless radiation intensity

$$I(t) \equiv \frac{3c^3 \bar{I}_S(t)}{2\mu_0^2 \omega_0^4 S^2 N^2}, \quad (44)$$

which reduces to the form

$$I(t) = [1 - As(t)]^4 w(t). \quad (45)$$

The typical behavior of solutions is shown in Figs. 1-4. The attenuation parameters are taken as $\gamma = 10$, $\gamma_1 = 10^{-3}$, $\gamma_3 = 1$, and the coupling parameter is $g = 100$. Different initial conditions are investigated and the anisotropy parameter (43) is varied. Note that, according to definitions (15) to (17), it should be: $w + s^2 \leq 1$. Therefore, we take the initial conditions that satisfy the relation $w_0 + s_0^2 = 1$. It is possible to separate four qualitatively different regimes.

Pure spin superradiance. Figure 1 presents the case of pure spin superradiance, when there is no initial coherence, $w_0 = 0$, and the system is fully polarized, $s_0 = 1$. Increasing the anisotropy shifts the curves to the right. It is interesting that the maximum of the radiation intensity increases with A , which is due to the greater contribution of the first factor in Eq. (45).

Spin subradiance. If there is no initial coherence imposed, $w_0 = 0$, and the system is not polarized at the initial time, $s_0 = -1$, then the values of the solutions are much smaller and the maximal radiation intensity is an order smaller than in the previous case of the polarized sample. This is shown in Fig. 2. A temporary radiation pulse happens because of the spin motion caused by spin interactions with each other and with the feedback field, though this radiation is very weak.

Spin induction. When one imposes on the system strong initial coherence, $w_0 = 1$, with no polarization, $s_0 = 0$, then the regime of spin induction is realized, as is illustrated in Fig. 3. The variation of the anisotropy does not influence much the behavior of w and s , but essentially increases the radiation intensity, with increasing A , and shifts the radiation maximum to nonzero time. While in the absence of anisotropy, the maximum of radiation intensity is at the initial time $t = 0$.

Triggered spin superradiance. The intermediate situation, shown in Fig. 4, corresponds to triggered spin superradiance, when there exists an essential initial polarization, $s_0 = 0.9$, and the spin motion is triggered by an initial coherent pulse, $w_0 = 0.19$. The maximum of the radiation intensity again becomes larger, when increasing A .

These results demonstrate that an ensemble of nanoclusters can produce coherent radiation. When coherence is imposed on the sample at the initial moment of time, the regimes of spin induction or triggered superradiance are produced. But, what is more important, it is feasible to realize such a setup, when the regime of pure spin superradiance can be achieved, as is illustrated in Fig. 1.

5 Typical properties of nanoclusters

Now we need to understand whether there really exist nanoclusters for which superradiance could be realized. As has been stressed above, nanoparticles possess rather strong magnetic anisotropy that is usually characterized by the anisotropy parameters, whose relation with the parameters, discussed in Sec. 2, is as follows:

$$K_1 = \frac{DS^2}{V_1}, \quad K_2 = \frac{D_2S^2}{V_1}, \quad K_4 = \frac{D_4S^4}{V_1},$$

where V_1 is the volume of a single nanoparticle. Respectively,

$$D = \frac{K_1 V_1}{S^2}, \quad D_2 = \frac{K_2 V_1}{S^2}, \quad D_4 = \frac{K_4 V_1}{S^4}.$$

The density of a single cluster is $\rho_1 = N_1/V_1$, with N_1 being the number of atoms composing the cluster. The total spin of a cluster is proportional to the number of atoms, $S \sim N_1$. Therefore the reduced anisotropy parameters are

$$D \sim \frac{K_1}{\rho_1 N_1}, \quad D_2 \sim \frac{K_2}{\rho_1 N_1}, \quad D_4 \sim \frac{K_4}{\rho_1 N_1^3}.$$

There exists a great variety of clusters with different properties [47,48]. Below, we shall discuss some of them in more detail.

Co clusters [56,57]. The coherence radius R_{coh} , below which coherent rotation of magnetization takes place, is $R_{coh} \approx 10$ nm. The radii below which particles are single-domain are about three times larger. But of the major importance for us is the coherence radius. The usual radius of a single cluster is $R \approx 1 - 2$ nm, containing the number of cobalt atoms $N_1 \approx 1000 - 1500$, the cluster volume being $V_1 \approx 2 \times 10^{-20}$ cm³. The anisotropy parameters

$$\begin{aligned} K_1 &= 0.22 \text{ MJ/m}^3 = 2.2 \times 10^6 \text{ erg/cm}^3, \\ K_2 &= 0.09 \text{ MJ/m}^3 = 0.9 \times 10^6 \text{ erg/cm}^3, \\ K_4 &= -0.01 \text{ MJ/m}^3 = -0.1 \times 10^6 \text{ erg/cm}^3 \end{aligned}$$

are caused by shape anisotropy, magnetocrystalline anisotropy, and surface anisotropy. The magnetic moment is well defined below the blocking temperature $T_B \approx 14$ K.

Fe clusters [57]. The coherence radius is $R_{coh} \approx 7.5$ nm. The number of iron atoms in a cluster is $N_1 \approx 1000$. The typical size of a single cluster is similar to that of a Co cluster. The anisotropy parameters are

$$K_1 = 0.32 \text{ MJ/m}^3 = 3.2 \times 10^6 \text{ erg/cm}^3, \quad K_4 = 0.05 \text{ MJ/m}^3 = 0.5 \times 10^6 \text{ erg/cm}^3,$$

with $K_2 \approx 0$.

Ni clusters [58]. The average radii of clusters are $R \approx 3 - 4$ nm. The blocking temperature is $T_B \approx 20 - 40$ K. Magnetic anisotropy is characterized by $K_1 = 1.5 \times 10^6$ erg/cm³.

CoAg clusters [57]. The characteristic radii are close to those of the above clusters. Anisotropy parameters are

$$K_1 = 0.02 \text{ MJ/m}^3 = 2 \times 10^5 \text{ erg/cm}^3, \quad K_2 = 0.006 \text{ MJ/m}^3 = 0.6 \times 10^5 \text{ erg/cm}^3.$$

Similar anisotropy parameters characterize CoNb and CoPt clusters [57], with the blocking temperature of order 100 K.

CoFe₂O₄ clusters [59]. Typical cluster radii can vary in the range of 1 - 10 nm. Depending on the radius of a cluster, its anisotropy parameters can be as follows:

$$\begin{aligned} K_1 &= 1.9 \times 10^7 \text{ erg/cm}^3 & (R = 2.85 \text{ nm}), \\ K_1 &= 1.4 \times 10^7 \text{ erg/cm}^3 & (R = 3.50 \text{ nm}), \end{aligned}$$

$$K_1 = 2.5 \times 10^6 \text{erg/cm}^3 \quad (R = 6.35 \text{ nm}) ,$$

The blocking temperature is about 200 – 300 K.

Fe₃O₄ clusters [60]. This material is called magnetite. Clusters are of the radius $R \approx 2 - 3$ nm. The magnetic anisotropy is

$$K_1 = 0.36 \text{ MJ/m}^3 = 3.6 \times 10^6 \text{erg/cm}^3 .$$

The blocking temperature is $T_B \approx 45$ K.

There exist many other clusters [47,48,61] with a variety of properties. For estimates, we shall take the values typical of Co, Fe, and Ni clusters. The coherence radius for these clusters is $R_{coh} = 10 - 100$ nm. Respectively, the number of atoms in a cluster of 10 nm is $N_1 \sim 10^5$, while in a cluster of 100 nm, it is $N_1 \sim 10^8$. The standardly prepared clusters have the radii $R \sim 1 - 3$ nm. The corresponding cluster volume is $V_1 \sim 10^{-20} \text{ cm}^3$. The number of atoms in a cluster is $N_1 \sim 10^3$. The related density inside a cluster is $\rho_1 \sim 10^{23} \text{ cm}^{-3}$. The cluster spin is $S \sim 10^3 - 10^5$, which gives the magnetic moment of the order of $10^3 - 10^5 \mu_B$. The blocking temperature, when thermally activated reversals are suppressed is $T_B \sim 10 - 100$ K. The magnetic anisotropy parameters are $K_1 \sim K_2 \sim 10^6 \text{ erg/cm}^3$, while K_4 is an order smaller. The reduced anisotropy parameters are $D \sim D_2 \sim 10^{-20} \text{ erg}$, while $D_4 \sim 10^{-27} \text{ erg}$. The ensemble of clusters is placed in a matrix, so that the density of clusters is $\rho \sim 10^{20} \text{ cm}^{-3}$.

Using these values gives for the anisotropy frequencies (21), (22), and (23) $\omega_D \sim \omega_2 \sim \omega_A \sim 10^{10} \text{ 1/s}$. This corresponds to the anisotropy field $B_D \equiv \omega_D/\gamma_e$. With $\gamma_e \sim 10^7 \text{ 1/G s}$, $\mu_0 \sim 10^{-20} \text{ erg/G}$, and $\text{G}^2 = \text{erg/cm}^3$, we have $B_D \sim 10^3 \text{ G}$. The feedback rate (28) is $\gamma_0 \sim 10^{10} \text{ 1/s}$. The dephasing rate, defined in Eq. (18), is $\gamma_2 \sim 10^{10} \text{ 1/s}$. As we see, the anisotropy frequencies are of the order of the attenuation rates γ_0 and γ_2 , and the anisotropy parameter (43) is $A \sim 0.1$. Therefore the resonance conditions (32) can already be satisfied for the Zeeman frequency (6) about $\omega_0 \sim 10^{11} \text{ 1/s}$. For this purpose, it is sufficient to have an external magnetic field $B_0 \sim 1 \text{ T}$. The wavelength, corresponding to this ω_0 is $\lambda \sim 1 \text{ cm}$. The mean intercluster distance is $a = 1/\rho^{1/3} \sim 10^{-7} \text{ cm}$. Hence $\lambda \gg a$, and the employed mean-field approximation is well justified.

The maximal radiation intensity, for the accepted parameters can reach very high values $I_S \sim 10^{19} \text{ erg/s}$, that is, $I_S \sim 10^{12} \text{ W}$. The superradiance pulse is very short, being $t_p \sim 1/g\gamma_2$. Here it is $t_p \sim 10^{-12} \text{ s}$. But it could be made much shorter, since the coupling parameter (35) is of the order $g \sim \omega_0/\gamma$, hence, diminishing the resonator damping γ the pulse duration could be made $\ll 10^{-12} \text{ s}$.

In conclusion, we have demonstrated that, despite the presence of anisotropy, strong dipole dephasing interactions, and nonuniform sizes, it is feasible to organize such a setup, when an ensemble of nanoclusters would produce a short superradiant pulse of high intensity. The developed theory is based on a microscopic Hamiltonian and the analysis involves realistic parameters typical of many magnetic nanoclusters. Fast polarization reversal of magnetic nanoclusters can find many applications, e.g., in magnetic recording [62,63], for magnetization-reversal measurements with micro-SQUID techniques [64], in quantum information processing, quantum computing, and for creating quantum artificial intelligence [65].

Acknowledgement. Financial support from the Russian Foundation for Basic Research is appreciated.

References

- [1] L. Allen and J.H. Eberly, *Optical Resonance and Two-Level Atoms* (Wiley, New York, 1975).
- [2] A.V. Andreev, V.I. Emelyanov, and Y.A. Ilinski, *Cooperative Effects in Optics* (Institute of Physics, Bristol, 1993).
- [3] L. Mandel and E. Wolf, *Optical Coherence and Quantum Optics* (Cambridge University, Cambridge, 1995).
- [4] M.G. Benedict, A.M. Ermolaev, V.A. Malyshev, I.V. Sokolov, and E.D. Trifonov, *Superradiance-Multiatomic Coherent Emission* (Institute of Physics, Bristol, 1996).
- [5] A.A. Kalachev and V.V. Samartsev, *Coherent Phenomena in Optics* (Kazan University, Kazan, 2003).
- [6] V.I. Yukalov and E.P. Yukalova, *Phys. Rev. B* **81**, 075308 (2010).
- [7] A.N. Poddubny, M.M. Glazov, and N.S. Averkiev, *Phys. Rev. B* **82**, 205330 (2010).
- [8] N.N. Bogolubov, M.T. Turaev, A.S. Shumovsky, and V.I. Yukalov, *Part. Nucl. Lett.* **9**, 5 (1985).
- [9] E.K. Bashkirov, A.S. Shumovsky, and V.I. Yukalov, *Phys. Dokl.* **30**, 367 (1985).
- [10] N.N. Bogolubov, M.T. Turaev, A.S. Shumovsky, and V.I. Yukalov, *Part. Nucl. Lett.* **14**, 33 (1996).
- [11] A.A. Bakasov and V.I. Yukalov, *Theor. Math. Phys.* **72**, 773 (1988).
- [12] A.A. Bakasov, N.N. Bogolubov, A.S. Shumovsky, and V.I. Yukalov, *Theor. Math. Phys.* **72**, 987 (1987).
- [13] V.I. Yukalov and E.P. Yukalova, *Laser Phys. Lett.* **2**, 302 (2005).
- [14] V.I. Yukalov, *Laser Phys. Lett.* **2**, 356 (2005).
- [15] N. Bloembergen and R.V. Pound, *Phys. Rev.* **95**, 8 (1954).
- [16] J.F. Kiselev, A.F. Prudkoglyad, A.S. Shumovsky, and V.I. Yukalov, *Mod. Phys. Lett. B* **1**, 409 (1988).
- [17] Y.F. Kiselev, A.F. Prudkoglyad, A.S. Shumovsky, and V.I. Yukalov, *J. Exp. Theor. Phys.* **67**, 413 (1988).
- [18] Y.F. Kiselev, A.F. Prudkoglyad, A.S. Shumovsky, and V.I. Yukalov, in: *Problems of Quantum Optics*, edited by V.I. Yukalov (JINR, Dubna, 1988), p. 68.
- [19] Y.F. Kiselev, A.S. Shumovsky, and V.I. Yukalov, *Mod. Phys. Lett.* **3**, 1149 (1989).
- [20] N.A. Bazhanov, D.S. Bulyanitsa, A.I. Zaitsev, A.I. Kovalev, V.A. Malyshev, and E.D. Trifonov, *J. Exp. Theor. Phys.* **70**, 1128 (1990).

- [21] L. Reichertz, H. Dutz, S. Goertz, D. Kramer, W. Meyer, G. Reicherz, W. Tiel, and A. Thomas, Nucl. Instrum. Meth. Phys. Res. A **340**, 278 (1994).
- [22] D.S. Bulyanitsa, A.V. Druzhin, and E.D. Trifonov, J. Exp. Theor. Phys. **118**, 273 (2000).
- [23] P. Bösiger, E. Brun, and D. Meier, Phys. Rev. A **18**, 671 (1978).
- [24] P. Bösiger, E. Brun, and D. Meier, Phys. Rev. A **20**, 1073 (1979).
- [25] R. Holzner, B. Derighetti, M. Ravani, and E. Brun, Phys. Rev. A **36**, 1280 (1987).
- [26] V.I. Yukalov, Phys. Rev. Lett. **75**, 3000 (1995).
- [27] V.I. Yukalov, Laser Phys. **5**, 526 (1995).
- [28] V.I. Yukalov, Laser Phys. **5**, 970 (1995).
- [29] V.I. Yukalov, Phys. Rev. B **53**, 9232 (1996).
- [30] V.I. Yukalov and E.P. Yukalova, Phys. Part. Nucl. **31**, 561 (2000).
- [31] V.I. Yukalov and E.P. Yukalova, Phys. Rev. Lett. **88**, 257601 (2002).
- [32] T.S. Belozerova, V.K. Henner, and V.I. Yukalov, Laser Phys. **2**, 545 (1992).
- [33] T.S. Belozerova, V.K. Henner, and V.I. Yukalov, Phys. Rev. B **46**, 682 (1992).
- [34] T.S. Belozerova, V.K. Henner, and V.I. Yukalov, Comput. Phys. Commun. **73**, 151 (1992).
- [35] J.T. Manassah, Laser Phys. **19**, 2102 (2009).
- [36] R. Friedberg and J.T. Manassah, Laser Phys. **20**, 250 (2010).
- [37] J.T. Manassah, Laser Phys. **20**, 259 (2010).
- [38] M.E. Taşgin, M.Ö. Oktel, L. You, and Ö.E. Müstecaplıoğlu, Laser Phys. **20**, 700 (2010).
- [39] O. Kahn, Molecular Magnetism (VCH, New York, 1995).
- [40] B. Barbara, L. Thomas, F. Lioni, I. Chiorescu, and A. Sulpice, J. Magn. Magn. Mater. **200**, 167 (1999).
- [41] V.I. Yukalov, Laser Phys. **12**, 1089 (2002).
- [42] V.I. Yukalov and E.P. Yukalova, Phys. Part. Nucl. **35**, 348 (2004).
- [43] V.I. Yukalov and E.P. Yukalova, Eur. Phys. Lett. **70**, 306 (2005).
- [44] V.I. Yukalov, Phys. Rev. B **71**, 184432 (2005).
- [45] V.I. Yukalov, V.K. Henner, and P.V. Kharebov, Phys. Rev. B **77**, 134427 (2008).

- [46] V.I. Yukalov, V.K. Henner, P.V. Kharebov, and E.P. Yukalova, *Laser Phys. Lett.* **5**, 887 (2008).
- [47] R.H. Kodama, *J. Magn. Magn. Mater.* **200**, 359 (1999).
- [48] G.C. Hadjipanayis, *J. Magn. Magn. Mater.* **200**, 373 (1999).
- [49] Y.F. Kisselev, *Phys. Part. Nucl.* **31**, 354 (2000).
- [50] E.C. Stoner and E.P. Wohlfarth, *Phil. Trans. Roy. Soc. London A* **240**, 599 (1948).
- [51] E.C. Stoner and E.P. Wohlfarth, *IEEE Trans. Magn.* **27**, 3475 (1991).
- [52] A. Thiaville, *J. Magn. Magn. Mater.* **182**, 5 (1998).
- [53] V.I. Yukalov, *Laser Phys.* **3**, 870 (1993).
- [54] N.N. Bogolubov and Y.A. Mitropolsky, *Asymptotic Methods in the Theory of Nonlinear Oscillations* (Gordon and Breach, New York, 1961).
- [55] E.A. Kochetov and V.I. Yukalov, *Laser Phys.* **5**, 186 (1995).
- [56] M. Jamet, W. Wernsdorfer, C. Thirion, D. Maily, V. Dupuis, P. Mélinon, and A. Pérez, *Phys. Rev. Lett.* **86**, 4676 (2001).
- [57] M. Jamet, W. Wernsdorfer, C. Thirion, V. Dupuis, P. Mélinon, A. Pérez, and D. Maily, *Phys. Rev. B* **69**, 024401 (2004).
- [58] G.F. Goya, F.C. Fonseca, R.F. Jardim, R. Muccillo, N.L. Carreno, E. Longo, and E.R. Leite, *J. Appl. Phys.* **93**, 6531 (2003).
- [59] T.E. Torres, A.G. Roca, M.P. Morales, A. Ibarra, C. Marquina, M.R. Ibarra, and G.F. Goya, *J. Phys. Conf. Ser.* **200**, 072101 (2010).
- [60] G.F. Goya and M.P. Morales, *J. Metast. Nanocryst. Mater.* **20**, 673 (2004).
- [61] S. Ostanin, S.S. Razee, J.B. Staunton, B. Ginatempo, and E. Bruno, *J. Appl. Phys.* **93**, 453 (2003).
- [62] G. Bate, *J. Magn. Magn. Mater.* **100**, 413 (1991).
- [63] D.J. Sellmyer, M. Yu, and R.D. Kirby, *Nanostruct. Mater.* **12**, 1021 (1999).
- [64] W. Wernsdorfer, D. Maily, and A. Benoit, *J. Appl. Phys.* **87**, 5094 (2000).
- [65] V.I. Yukalov and D. Sornette, *Laser Phys. Lett.* **6**, 833 (2009).

Figure Captions

Fig. 1. Regime of pure spin superradiance. Numerical solutions of Eqs. (40) for the coherence intensity $w(t)$, spin polarization $s(t)$, and the radiation intensity $I(t)$ as functions of time t (in units of $1/\gamma_2$). The attenuation parameters (in units of γ_2) are $\gamma = 10$, $\gamma_3 = 1$, and $\gamma_1 = 10^{-3}$. The coupling parameter is $g = 100$. The initial conditions are $w_0 = 0$ and $s_0 = 1$.

Fig. 2. Regime of spin subradiance. Coherence intensity $w(t)$, spin polarization $s(t)$, and radiation intensity $I(t)$ for the same system parameters, as in Fig. 1, but for the initial conditions $w_0 = 0$, $s_0 = -1$, corresponding to nonpolarized clusters.

Fig. 3. Regime of spin induction. Coherence intensity $w(t)$, spin polarization $s(t)$, and radiation intensity $I(t)$ for the same parameters, as in Fig. 1, but for the initial conditions $w_0 = 1$, $s_0 = 0$.

Fig. 4. Regime of triggered spin superradiance. Coherence intensity $w(t)$, spin polarization $s(t)$, and radiation intensity $I(t)$ for the same parameters, as in Fig. 1, but for the initial conditions $w_0 = 0.19$, $s_0 = 0.9$.

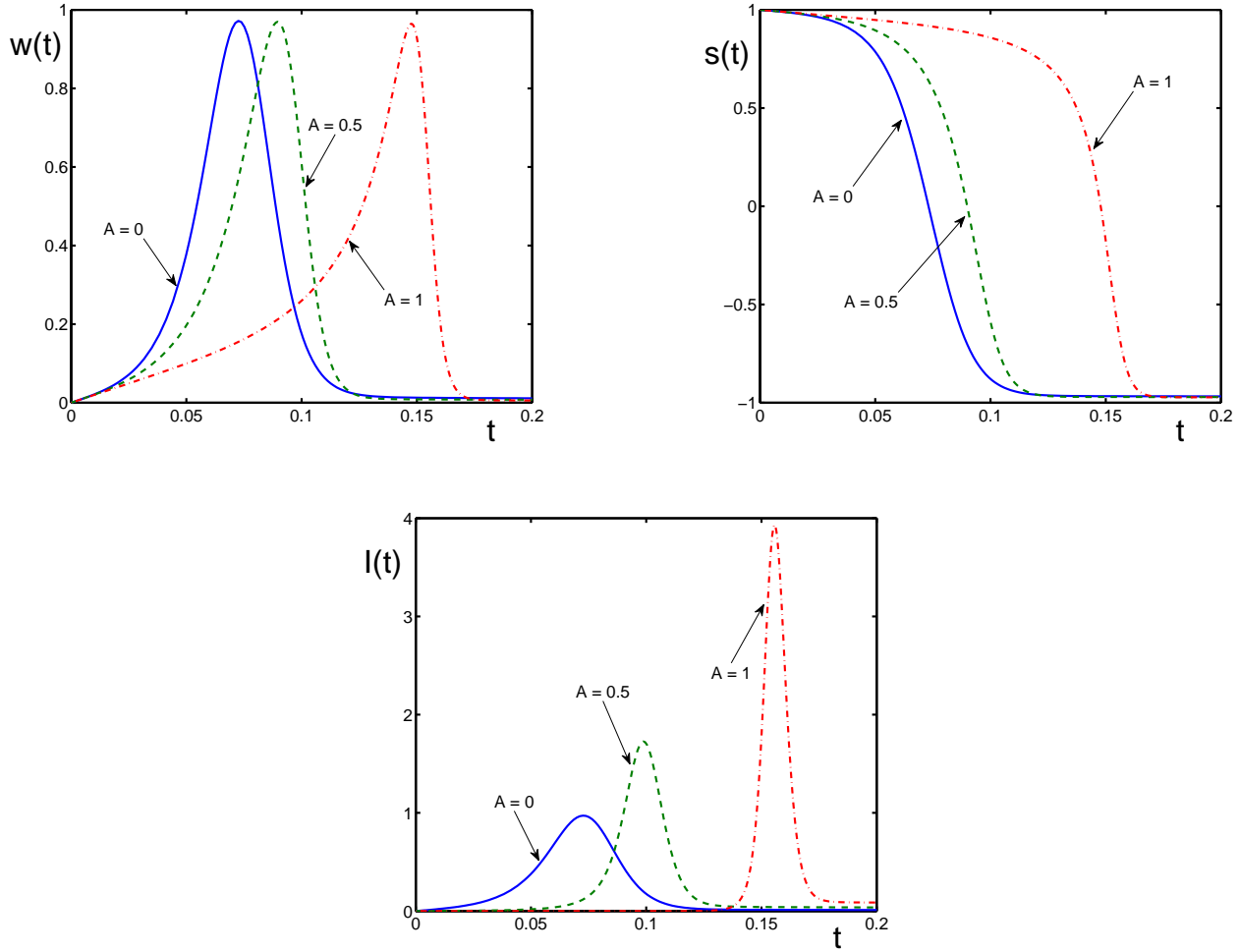


Figure 1: Regime of pure spin superradiance. Numerical solutions of Eqs. (40) for the coherence intensity $w(t)$, spin polarization $s(t)$, and the radiation intensity $I(t)$ as functions of time t (in units of $1/\gamma_2$). The attenuation parameters (in units of γ_2) are $\gamma = 10$, $\gamma_3 = 1$, and $\gamma_1 = 10^{-3}$. The coupling parameter is $g = 100$. The initial conditions are $w_0 = 0$ and $s_0 = 1$.

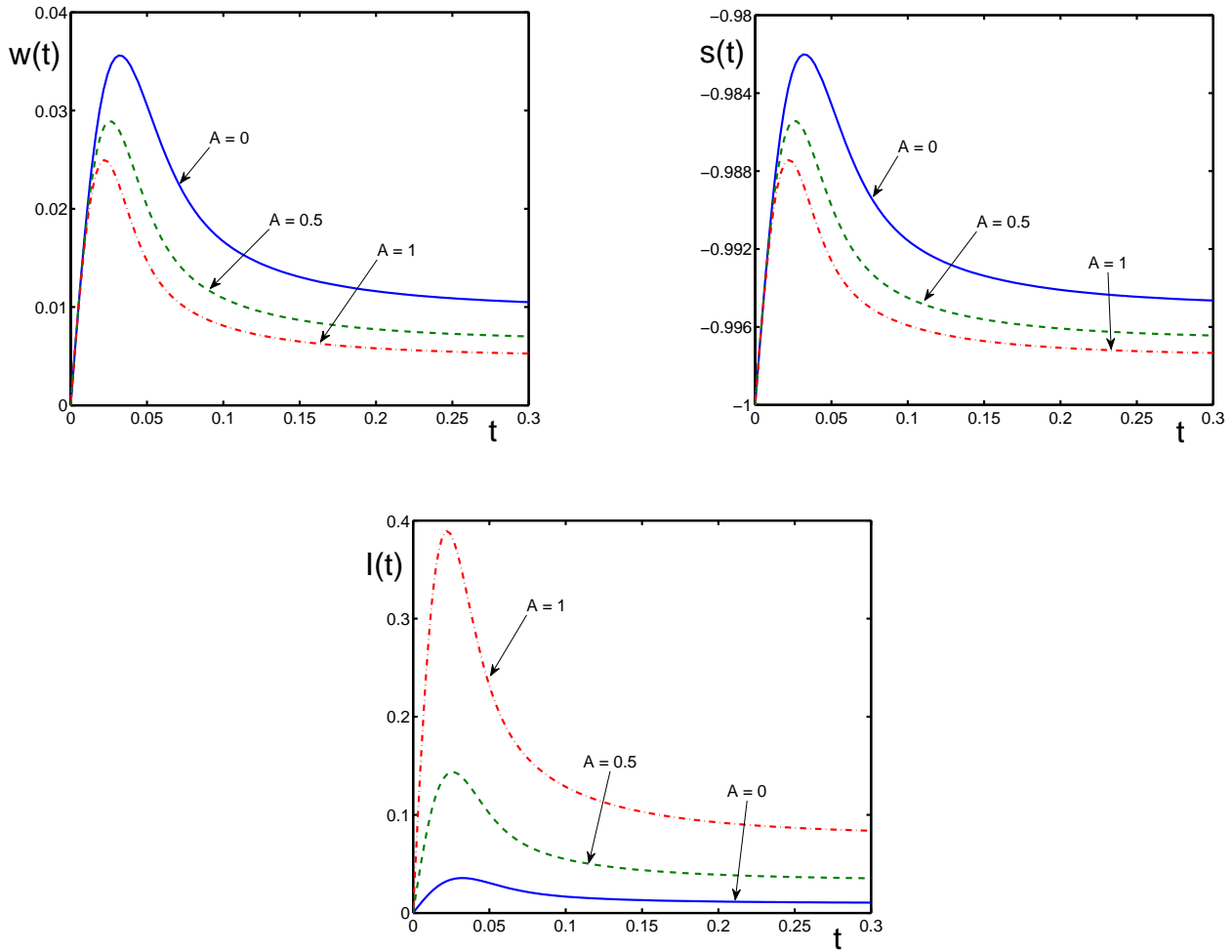


Figure 2: Regime of spin subradiance. Coherence intensity $w(t)$, spin polarization $s(t)$, and radiation intensity $I(t)$ for the same system parameters, as in Fig. 1, but for the initial conditions $w_0 = 0$, $s_0 = -1$, corresponding to nonpolarized clusters.

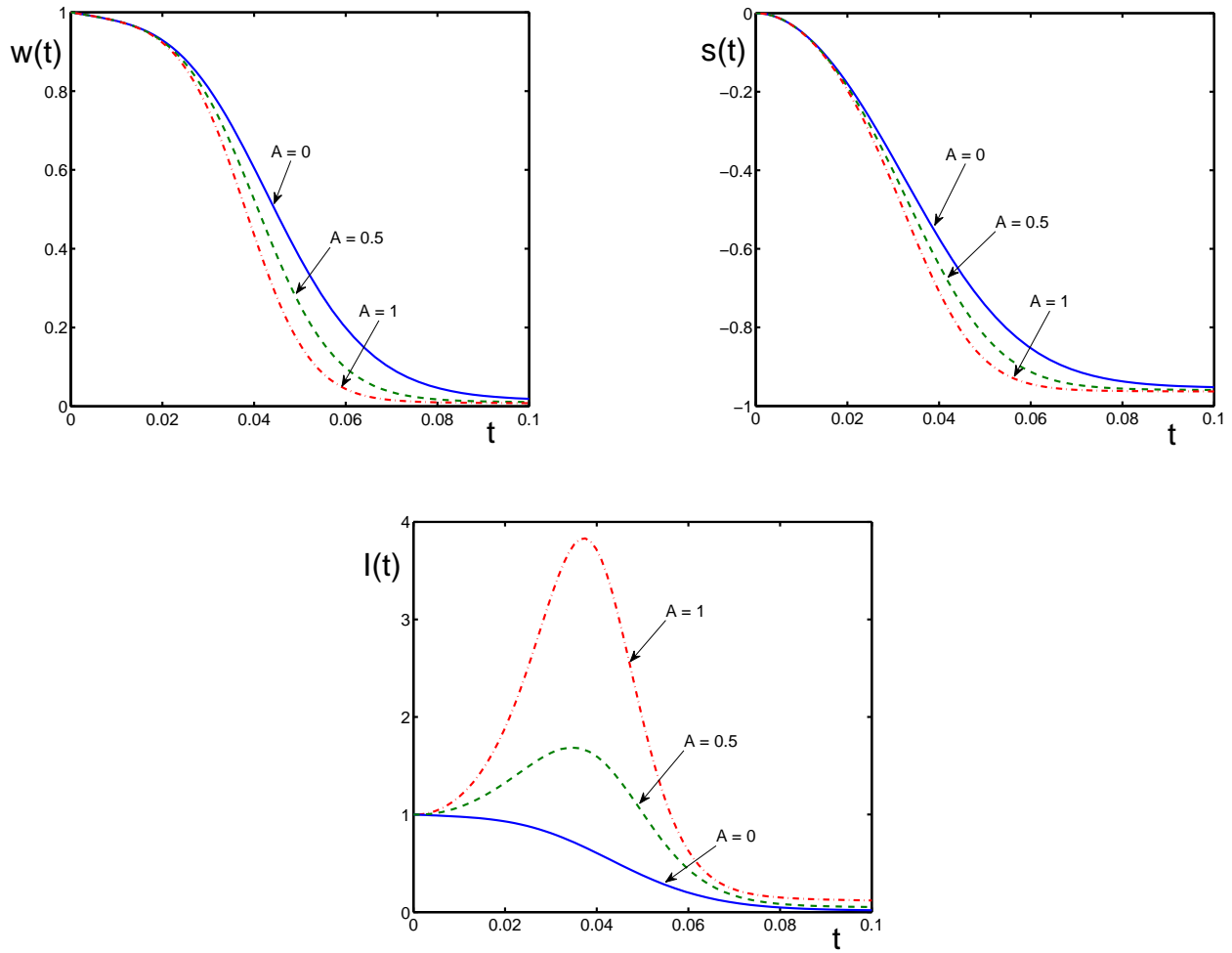


Figure 3: Regime of spin induction. Coherence intensity $w(t)$, spin polarization $s(t)$, and radiation intensity $I(t)$ for the same parameters, as in Fig. 1, but for the initial conditions $w_0 = 1$, $s_0 = 0$.

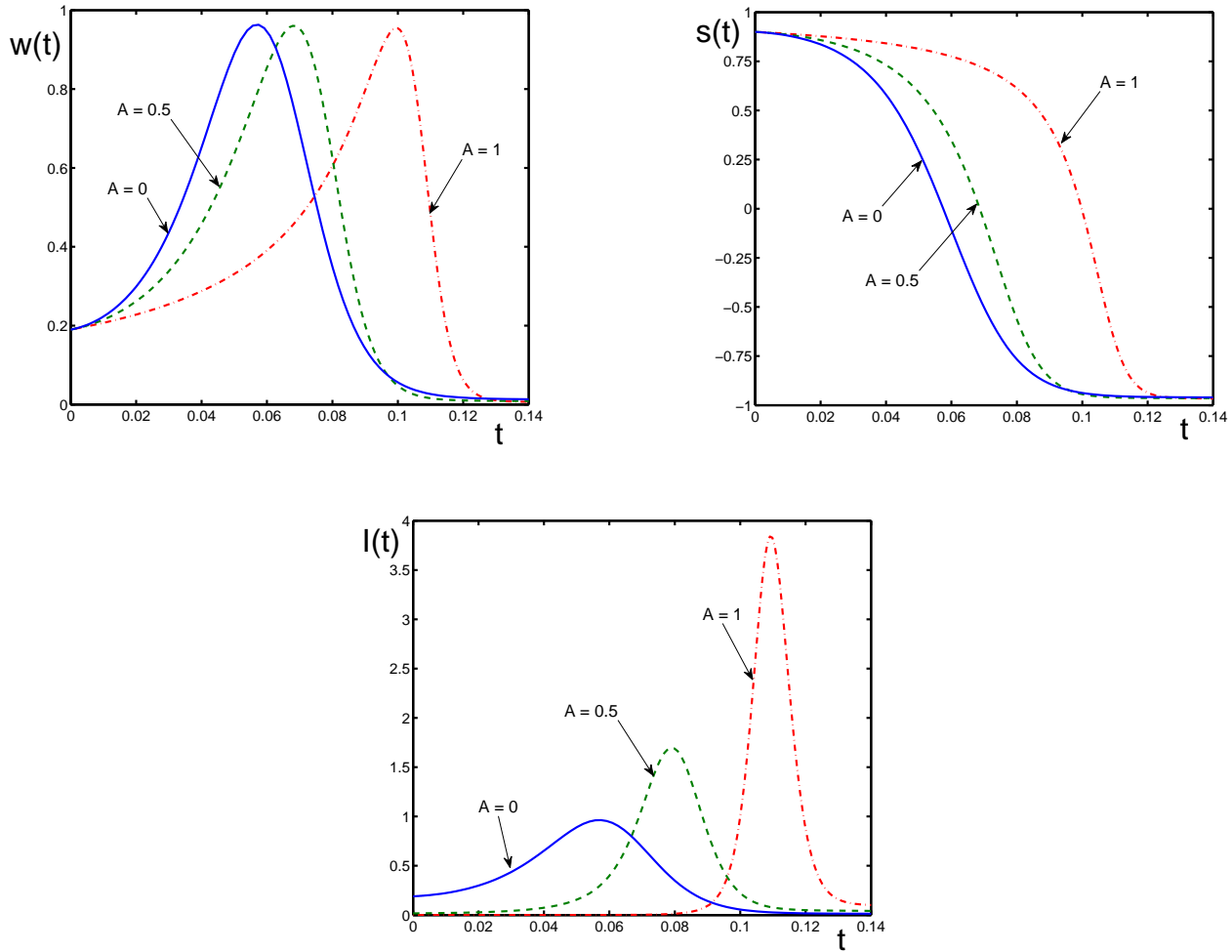


Figure 4: Regime of triggered spin superradiance. Coherence intensity $w(t)$, spin polarization $s(t)$, and radiation intensity $I(t)$ for the same parameters, as in Fig. 1, but for the initial conditions $w_0 = 0.19$, $s_0 = 0.9$.